Supplemental data

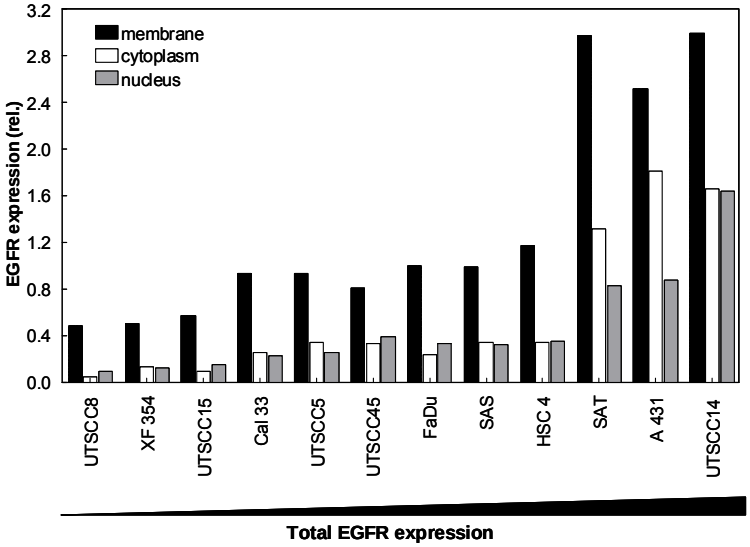

Figure 1: Distribution of EGFR within membranous, cytoplasmatic and nuclear cell extracts. Distribution has been determined by Western blot analysis of cell extracts made of 50,000 cells. The cellular expression level and distribution varies between the different cell lines; however, the membranous fraction always contained the major amount of EGFR molecules.

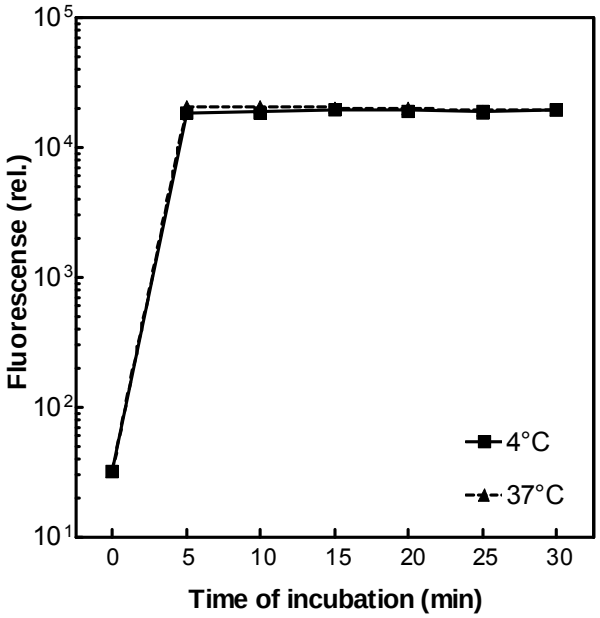

Figure 2: Cetuximab binding kinetics at 4°C and 37°C. Living single A431 cells expressing high EGFR were incubated at 4°C or 37°C with PBS containing 30 nM Cetuximab, washed, incubated with FITC conjugated anti human IgG, washed again and used for FACS analysis. FACS analysis was performed using 100,000 cells. During incubation with 30 nM Cetuximab the surface of A431 is saturated after 5 min. Incubation for longer periods does not result in further increase of molecules bound to the cell surface.

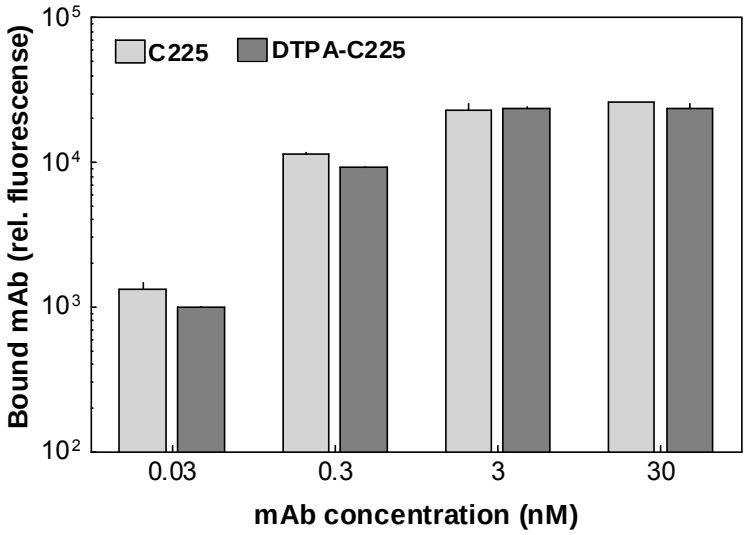

Figure 3: Affinity of Cetuximab (C225/light grey) and DTPA-Cetuximab (DTPA-C225/dark grey). mAb binding was measured by FACS analysis of 100,000 cells at various concentrations using FITC conjugated anti human IgG. A saturation of mAb binding can be seen at a concentration of 3 nM. A further increase of mAb concentration does not result in higher signal intensity. No significant reduction of affinity can be visualized between Cetuximab and DTPA-Cetuximab at saturating concentrations.

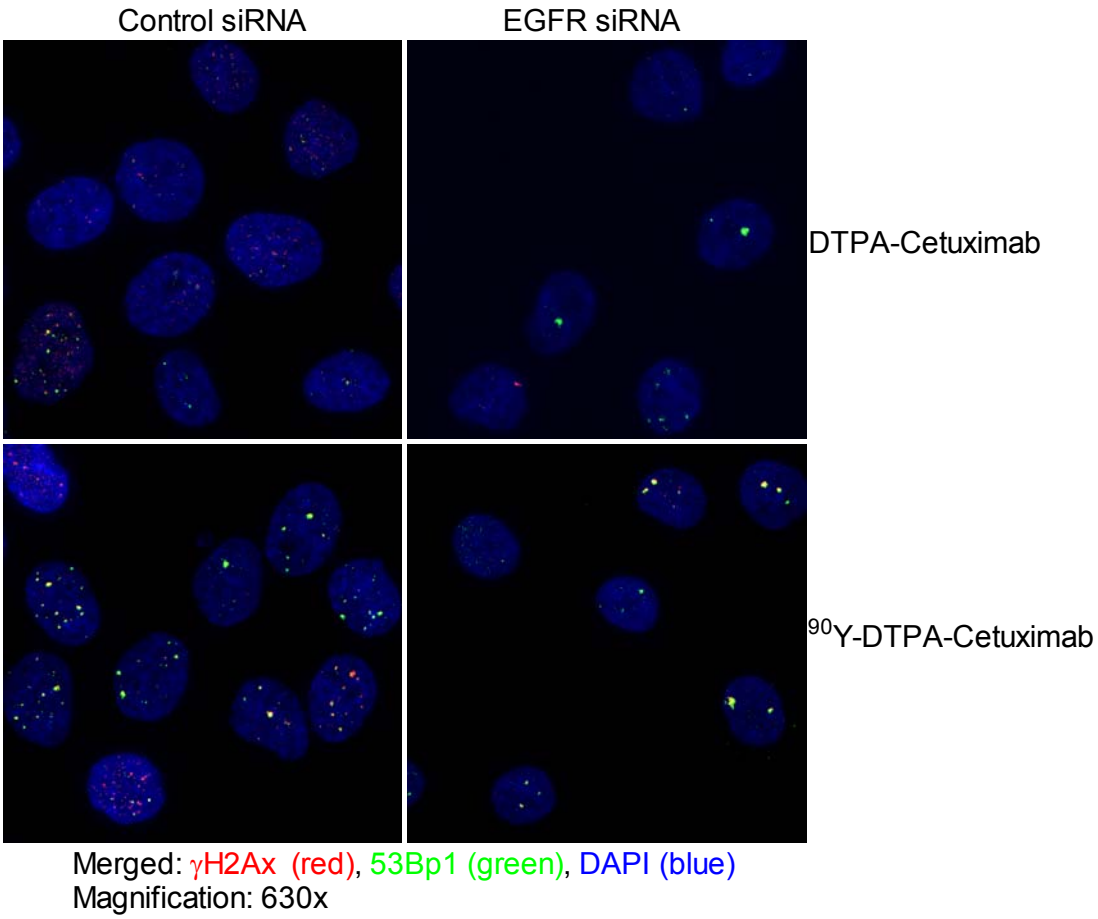

Figure 4: Accumulation of DSB repair foci in UTSCC14 cells in dependence of EGFR expression. Detection of γH2AX and 53Bp1 foci in cells treated with control siRNA or EGFR specific siRNA analyzed in Fig. 3D after 24h of ^{90}Y-DTPA-Cetuximab treatment. Representative merged pictures are shown in 630 x magnification.

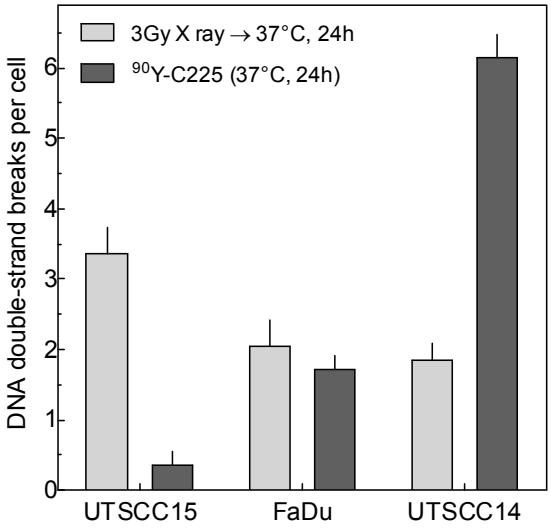

Figure 5: Number of DSB repair foci visualized 24 h after external irradiation with 3 Gy or Incubation with ^{90}Y-DTPA-Cetuximab (^{90}Y-C225) for 24 h. The number of DSBs was measured using γH2AX and 53Bp1 costaining. For X-irradiated cells there was a clear difference in the number of residual DSB repair foci indicating a strong difference in DSB repair capacity. For UT-SCC15 cells this number is 1.8 times higher than the respective number measured for UT-SCC14 cells.

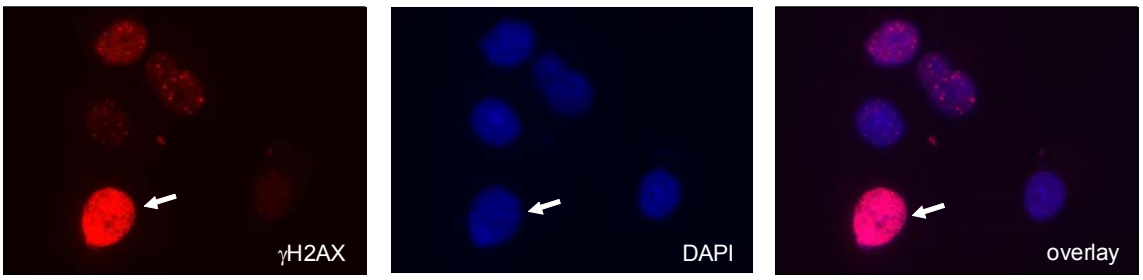

Figure 6: Pan-nuclear γH2AX staining in UT-SCC14 cells after 24 h treatment with ^{90}Y-DTPA-Cetuximab. Such pan-nuclear γH2AX staining is considered to be an indicator of apoptosis. The number of cells showing this phenotype was very low after treatment with ^{90}Y-DTPA-Cetuximab in all cell lines.

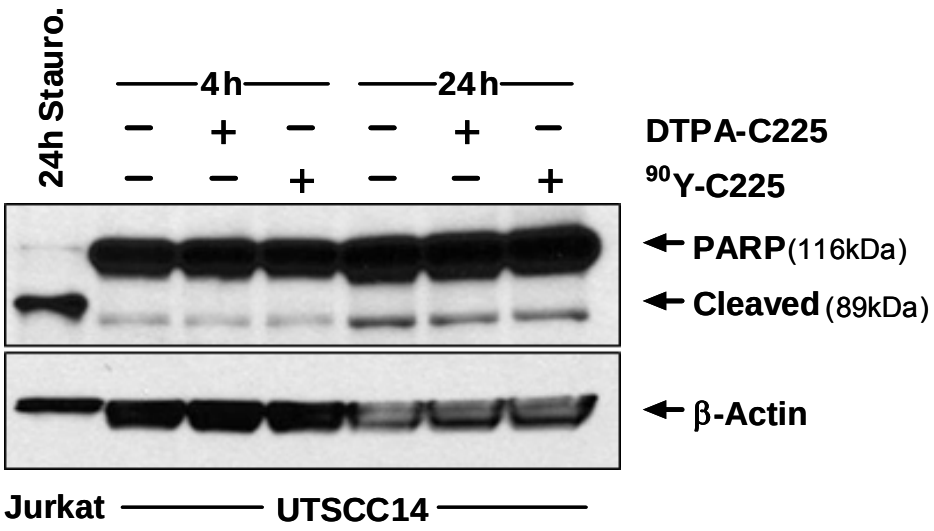

Figure 7: Detection of apoptosis via PARP cleavage. UT-SCC 14 cells were labeled with ^{90}Y-DTPA-Cetuximab for 5 min followed by an incubation at 37°C. After an incubation for 4 or 24 h cells were prepared for the detection of apoptosis via PARP cleavage.